Diffusion of small clusters on metal (100) surfaces: Exact master-equation analysis for lattice-gas models

J. R. Sanchez*
International Institute of Theoretical and Applied Physics, Iowa State University, Ames, Iowa 50011

J. W. Evans
Department of Mathematics and Ames Laboratory, Iowa State University, Ames, Iowa 50011
(Received 7 May 1998)

Exact results are presented for the surface diffusion of small two-dimensional clusters, the constituent atoms of which are commensurate with a square lattice of adsorption sites. Cluster motion is due to the hopping of atoms along the cluster perimeter with various rates. We apply the formalism of Titulaer and Deutch [J. Chem. Phys. **77**, 472 (1982)], which describes evolution in reciprocal space via a linear master equation with dimension equal to the number of cluster configurations. We focus on the regime of rapid hopping of atoms along straight close-packed edges, where certain subsets of configurations cycle rapidly between each other. Each such subset is treated as a single quasiconfiguration, thereby reducing the dimension of the evolution equation, simplifying the analysis, and elucidating limiting behavior. We also discuss the influence of concerted atom motions on the diffusion of tetramers and larger clusters. [S0163-1829(99)05704-5]

I. INTRODUCTION

There has long been interest in the diffusion of small two-dimensional (2D) metal adatom clusters on single crystal metal surfaces,[1] as this phenomenon has potential importance for both film growth and equilibration processes.[2,3] Direct field ion microscopy observations of small cluster diffusion[1] were used to assess diffusion coefficients D. This work also prompted some exact analyses of lattice-gas models for diffusion of very small clusters,[4,5] as well as the application of semiempirical methods to estimate energetic barriers for both conventional and different diffusion pathways.[6,7] Recent scanning tunneling microscopy studies[8–10] have revealed significant diffusion of large 2D clusters, with hundreds to thousands of atoms, on metal surfaces. The dependence of D on cluster size N (i.e., the number of atoms) was assessed and cluster diffusion and coalescence was shown to dominate adlayer coarsening in metal (100) homoepitaxial systems under certain conditions.[8,9] Kinetic Monte Carlo simulations of large cluster diffusion have also been utilized to examine the dependence of D on N for various mass transport pathways[6,11] and to examine correlations in the cluster's walk.[12] However, a comprehensive understanding of large cluster diffusion is still lacking.

The latter assessment motivates our return to the consideration of exact analytic treatments for the diffusion of small clusters. Such studies can provide a fundamental understanding of the dependence of cluster diffusivity on kinetic pathways (noting that diffusivity does not just depend on energetics or equilibrium properties), of correlations in cluster motion, etc. A key limitation, however, is that the size or complexity of these calculations increases in proportion to the number of possible configurations of the cluster C═C(N), which in turn increases exponentially with size N. Since this restricts such analyses to very small sizes, we naturally also explore ways to extend this approach at least to somewhat larger sizes.

In this paper we analyze the surface diffusion of small two-dimensional adatom clusters, where cluster motion is mediated by the hopping of atoms around the cluster perimeter. We restrict our attention to the case of clusters commensurately adsorbed on surfaces characterized by a square lattice of adsorption sites [e.g., unreconstructed fcc (100) or bcc (100) metal surfaces]. We determine the cluster diffusivity D in terms of the rates for various perimeter hopping processes. Our focus is on the limiting regime of rapid diffusion along straight close-packed edges, a scenario that should exist for most metal (100) systems. In this regime, certain subsets of cluster configurations cycle rapidly between each other and our analysis treats each such subset as a single quasiconfiguration. This both simplifies the analysis and helps to elucidate the limiting behavior. In Sec. II we describe our model for cluster diffusion and then present a master-equation formalism in Sec. III, which allows an exact analysis of the model. Explicit results for diffusion of monomers, dimers, trimers, tetramers, and pentamers are presented in Sec. IV for our basic model where only single atom hops are allowed. Refined models including concerted atom moves are discussed in Sec. V. A brief discussion of correlations in the walk of the cluster is presented in Sec. VI and we provide some concluding remarks in Sec. VII.

II. LATTICE-GAS MODELS FOR CLUSTER DIFFUSION

We first describe the type of models considered in this paper. Clusters are defined as groups of adatoms *connected* by nearest-neighbor (NN) bonds on a 2D lattice. We associate an energy with each cluster configuration of $E=-MJ$, where M denotes the number of NN bonds and $J>0$ gives the magnitude of an attractive pair-bond energy. Clusters can transform between such connected configurations as a result of various types of hops of perimeter atoms to adjacent or diagonally adjacent empty sites. The key observation here is that hops of the individual perimeter atoms lead to a shift of

 ©1999 The American Physical Society

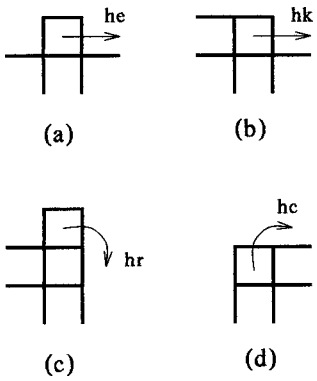

FIG. 1. Schematic of the key perimeter diffusion processes: (a) ''straight edge hopping,'' (b) ''kink escape,'' (c) ''corner rounding,'' and (d) ''core breakup.'' The squares in this and subsequent figures represent the individual atoms arranged on a square lattice of adsorption sites.

the center of mass of the whole cluster and thus to its diffusion. The feature that the atomic hop rates satisfy detailed balance implies that the equilibrium distribution of configurations is given by the Gibbs measure proportional to $\exp(-\beta E)$, *restricted* to the accessible subset of connected configurations. Here we set $\beta = 1/k_B T$, where T denotes the substrate temperature.

At least for larger clusters, it is natural to divide the above types of models into two basic categories, depending on whether or not the kinetic rules allow vacancies to diffuse through the interior of the cluster.[8–11] If they do, we are implicitly regarding the four atoms adjacent to the interior vacancy as ''perimeter'' atoms and the kinetic rules would allow one of them to exchange with the vacancy, thus facilitating its diffusion. Such models are traditionally placed in the so-called terrace diffusion (TD) class. If vacancies cannot diffuse through the cluster interior and thus only external perimeter atoms can move, then the model is traditionally placed in the so-called perimeter diffusion (PD) class. Traditional simplistic mean-field-type analyses of the dependence of cluster diffusion coefficient D on size N (for large N) suggest different behavior for the TD and PD classes.[8,11] However, it is clear that the actual behavior will depend strongly on the magnitude of the rate controlling bulk vacancy transport (relative to other rates) and on the size of the cluster. In our current studies, the clusters are sufficiently small that bulk vacancies cannot form, so cluster diffusion is unambiguously associated with the PD class.

In the basic model that we shall utilize to study small cluster diffusion, it is instructive to distinguish between the following specific types of adatom hops: (i) ''straight edge hopping'' of singly bonded atoms along straight close-packed edges at a rate h_e [Fig. 1(a)], which involves no net change in bonding or energy; (ii) ''corner rounding'' at rate h_r [Fig. 1(b)], which also involves no net change in bonding or energy [in metal (100) epitaxial systems, such moves actually occur in two distinct steps: a first hop to a diagonal or next NN site, followed by a more rapid return to the NN site; thus our model simplifies this two step process to a single step (and preserves NN connectivity)]; (iii) ''escape from kink sites'' at rate h_k [Fig. 1(c)], which involves a net breaking of one bond; and (iv) ''core breakup'' at rate h_c [Fig. 1(d)], which also involves a net breaking of one bond. This latter process is so named because it facilitates the breakup the ''rectangular core'' of a large cluster, which is necessary for true long-range diffusion of such clusters.[6,8]

Detailed balance requires that $h_k = \exp(-\beta J) h_e$ and $h_c = \exp(-\beta J) h_r$. For metal (100) systems, one typically expects that[6,8] $h_c \ll h_k \approx h_r \ll h_e$, so the rates are not simply related to either the initial number or the net change in the number of bonds for the atomic hop. For larger clusters, it is necessary to also consider the very slow ''edge breakout'' process of an atom from a straight edge, which involves a net breaking of two bonds. If the reverse corner rounding process is allowed, edge breakout must be included with a rate $h_b = \exp(-2\beta J) h_r$ in order to avoid violating detailed balance. However, for the small clusters considered here, the edge breakout process is not relevant (and, in practice, it may not be that important even for diffusion of larger clusters).

Various other modifications to this basic model might be appropriate for a more realistic description of actual metal (100) systems. Most involve the introduction of concerted moves of more than one perimeter adatom. ''Dimer shearing'' in square tetramers, wherein a pair of atoms on one side of a square tetramer shears relative to the other pair, has been recently identified as playing an important role in tetramer diffusion. Other possibilities include ''dimer edge hopping'' and ''trimer edge hopping'' along straight edges and ''dimer kink escape,'' some of which can also be important. See Ref. 7 and Sec. V. Another possibility is ''efficient'' corner rounding via a concerted exchange process. This is perhaps more likely at kink sites along otherwise straight edges (''local corners'') than at ''global'' corners or extremities of large rectangular clusters.

III. ANALYTIC MASTER-EQUATION FORMALISM

A. Basic formalism

We review and refine the formalism of Titulaer and Deutsch,[5] which provides an analytic treatment of cluster diffusion in the types of PD or TD models discussed in Sec. II. Here the number of particles N in the cluster is fixed, as is the number C of accessible cluster configurations (different shapes and orientations). We label these configurations by $s,t,v,\ldots$ with energies $E_s, E_t, E_v, \ldots$, respectively. Perimeter hopping of atoms produces transitions between certain pairs of configurations, say, from s to t with a rate h_{ts} and a corresponding displacement of the center of mass of the cluster by $\boldsymbol{\rho}_{ts}$. The rates h_{ts} satisfy detailed-balance conditions $h_{ts}\exp(-\beta E_s) = h_{st}\exp(-\beta E_t)$. The probability $P_s(\mathbf{r},\tau)$ of finding the cluster in configuration s, with the center of mass at position $\mathbf{r}$ (measured in units of the lattice spacing), at time τ, satisfies the master equation

$$\frac{d}{d\tau} P_s(r,\tau) = \sum_{t,s} \left[h_{st} P_t(\mathbf{r} - \boldsymbol{\rho}_{st,}\tau) - h_{ts} P_s(\mathbf{r},\tau) \right]. \quad (1)$$

We caution that if the s configuration at $\mathbf{r}$ can be obtained from several t configurations with distinct locations (or, equivalently, if the s configuration at $\mathbf{r}$ can transform to several t configurations with distinct locations), then t will appear a corresponding number of times in the sum with the appropriate $\boldsymbol{\rho}_{ts}$. It should be noted that the possible locations

r of the cluster center of mass lie on a discrete lattice that is ''finer'' than the original lattice of adsorption sites.

Fourier transformation $\hat{P}_s(\mathbf{k},\tau)=\Sigma_{\mathbf{r}}\exp(-i\mathbf{k}\cdot\mathbf{r})P_s(\mathbf{r},\tau)$ naturally deconvolutes the spatial coupling in Eq. (1) and reduces the master equations to a simpler C-dimensional linear evolution equation. Note that $\hat{P}_s(\mathbf{k}=0,\tau)$ gives the *total population* $P_s(\tau)$ of clusters with configuration s at time τ. In terms of the vector $\hat{\mathbf{P}}(\mathbf{k},\tau)$ with components $[\hat{\mathbf{P}}(\mathbf{k},\tau)]_s=\hat{P}_s(\mathbf{k},\tau)$, one obtains

$$\frac{d}{d\tau}\hat{\mathbf{P}}(\mathbf{k},\tau)=\underline{\underline{M}}(\mathbf{k})\cdot\hat{\mathbf{P}}(\mathbf{k},\tau), \tag{2}$$

where $[\underline{\underline{M}}(\mathbf{k})]_{st}=h_{st}\exp(-i\mathbf{k}\cdot\boldsymbol{\rho}_{st})$ for $s\neq t$ and $-\Sigma_{v\neq s}h_{vs}$ for $s=t$, with appropriate modifications where multiple transitions between s and t or v' are possible. All the eigenvalues $\lambda_i(\mathbf{k})$ (with $0\leq i\leq C-1$) of $\underline{\underline{M}}(\mathbf{k})$ are real and negative for $k=|\mathbf{k}|>0$. There is a single ''acoustic branch'' $i=0$, say, for which $\lambda_0(\mathbf{k})\sim Ak^2$ vanishes as $k\to 0$.[5] Let $\boldsymbol{\Phi}_i$ and $\boldsymbol{\vartheta}_i^T$ denote the biorthonormal right and left ith eigenvectors of $\underline{\underline{M}}(\mathbf{k})$, respectively, so that $\boldsymbol{\vartheta}_i^T\cdot\boldsymbol{\Phi}_j=\delta_{i,j}$. Then $\underline{\underline{Q}}_j(\mathbf{k})=\boldsymbol{\Phi}_i\boldsymbol{\vartheta}_i^T$ denotes the projector onto the ith eigenspace of $\underline{\underline{M}}(\mathbf{k})$ and the solution to Eq. (2) has the form

$$\hat{\mathbf{P}}(\mathbf{k},\tau)=\exp[\underline{\underline{M}}(\mathbf{k})\tau]\cdot\hat{\mathbf{P}}(\mathbf{k},0)$$

$$=\sum_{i\geq 0}\exp[\lambda_i(\mathbf{k})\tau]\underline{\underline{Q}}_i(\mathbf{k})\cdot\hat{\mathbf{P}}(\mathbf{k},0). \tag{3}$$

Some minor modification to this formulation is required for monomers since atomic hops lead to transitions to the same configuration, in contrast to clusters with $N>1$.

We shall see below that the behavior of $\hat{\mathbf{P}}(\mathbf{k},\tau)$ for small $\mathbf{k}$ is of primary interest in the context of diffusion. Since only $\lambda_0(\mathbf{k})\to 0$ as $\mathbf{k}\to 0$, it follows from Eq. (3) that for *small* k one has

$$\hat{\mathbf{P}}(\mathbf{k},\tau)\sim\exp[\lambda_0(\mathbf{k})\tau]\underline{\underline{Q}}_0(\mathbf{k})\cdot\hat{\mathbf{P}}(\mathbf{k},0),\quad\text{as}\quad\tau\to\infty. \tag{4}$$

From the properties of $\underline{\underline{M}}$ and the detailed-balance condition on h_{st}, it follows that $\boldsymbol{\vartheta}_0^T\to\mathbf{E}^T=(1,1,1,\ldots)$ and $\boldsymbol{\Phi}_0\to\mathbf{P}^{\mathrm{eq}}$ as $k\to 0$, where $[\mathbf{P}^{\mathrm{eq}}]_s=\exp(-\beta E_s)/Z$, with $Z=\Sigma_s\exp(-\beta E_s)$. Thus the projector onto the ''acoustic'' eigenspace satisfies $\underline{\underline{Q}}_0(\mathbf{k})\to\mathbf{P}^{\mathrm{eq}}\mathbf{E}^T$ as $k\to 0$.[13]

Finally, we determine the cluster diffusion coefficient D defined in terms of the motion of the cluster center of mass **r** via the standard formula $\langle\mathbf{r}\cdot\mathbf{r}\rangle\sim 4D\tau$ as $\tau\to\infty$. By symmetry, the x and y components of the center of mass thus satisfy $\langle x^2\rangle\sim\langle y^2\rangle\sim 2D\tau$ as $\tau\to\infty$. If $\mathbf{k}=(k_x,k_y)$ so that $k^2=k_x^2+k_y^2$, then these quantities can be readily obtained as

$$\langle x^2\rangle=\partial^2/\partial(ik_x)^2\sum_s\hat{P}_s(\mathbf{k},\tau)|_{\mathbf{k}=\mathbf{0}}$$

$$\langle y^2\rangle=\partial^2/\partial(ik_y)^2\sum_s\hat{P}_s(\mathbf{k},\tau)|_{\mathbf{k}=\mathbf{0}}. \tag{5}$$

Now, using Eq. (4) and the other results for small **k** behavior, one has that[14]

$$D=\tfrac{1}{4}\partial^2/\partial(i\mathbf{k})^2\lambda_0(\mathbf{k})|_{\mathbf{k}=\mathbf{0}}. \tag{6}$$

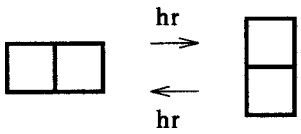

FIG. 2. Configurations and transition rates for dimer diffusion.

Thus D can be obtained directly from an analysis of the acoustic eigenvalue of $\underline{\underline{M}}(\mathbf{k})$.

B. Quasiconfigurations for rapid edge diffusion

As noted in Sec. I of this paper, we are particularly interested in the limiting behavior in the regime of rapid straight edge hopping, i.e., large h_e. This regime is often of most physical relevance for metal (100) systems. Our strategy here will be to replace several isoenergetic configurations of the cluster, which rapidly interconvert via straight edge hopping processes, by a single quasiconfiguration. Specific examples are given in Sec. IV. Within the above formalism, this not only reduces the dimension of configuration space and thus the complexity of the analysis, but also provides greater insight into the behavior in this regime. It is only necessary to make the following minor refinements in applying the above formalism: (i) the center of mass for each quasiconfiguration is determined from a simple average of the center-of-mass locations of the constituent configurations and the $\boldsymbol{\rho}_{ts}$ are calculated accordingly and (ii) the rate of transition from a quasiconfiguration to some other configuration equals the product of the rate for the appropriate atomic hop facilitating this transition and the probability that the quasiconfiguration is in the appropriate initial configuration. For the latter, one simply recognizes that the quasiconfiguration has an equal probability of being in any of its isoenergetic constituent configurations. Again, specific examples will be given in the following section.

IV. RESULTS FOR CLUSTER DIFFUSION VIA PD WITH SINGLE-ATOM HOPS

The formalism of Sec. III is now applied to calculate diffusion coefficients D for clusters of size $N=1-5$ on a square lattice. In the discussion and figures below, specified rates refer to transitions from a specific s configuration to a specific t configuration with specific relative displacement (rather than the total rate for transitions to all possible t configurations). Further details of the calculations, including center-of-mass displacements, are given in the Appendix.

A. Monomer diffusion

Diffusion of a monomer (which has a single configuration, so $C=1$) constitutes the classic example of a ''pure'' random walk in a discrete lattice model. If h_0 is the rate for the monomer to hop to each adjacent site, then it can be readily shown that $\langle x^2\rangle=\langle y^2\rangle=2h_0\tau$ for all τ, so $D=h_0$.

B. Dimer diffusion

Here there are two configurations (horizontal and vertical), so $C=2$. The only operative hopping process is corner rounding, which leads to transitions between horizontal and vertical configurations (see Fig. 2). Since for each step in the

dimer's motion there are four possible equally likely displacements of its center of mass by $(\pm\frac{1}{2},\pm\frac{1}{2})$, the dimer's motion is also a pure random walk.[12] In comparison with monomer diffusion, it readily follows that $\langle x^2\rangle=\langle y^2\rangle=h_r\tau$ for all τ, so $D=h_r/2$.

C. Trimer diffusion

Here there are six configurations (two linear and four bent), so $C=6$. These configurations are indicated in Fig. 3, as well as possible transitions between them and the associated transition rates. Both straight edge diffusion and corner rounding are operative, where the latter is expected to be rate limiting. Clearly, the six configurations occur with equal probability as $\tau\to\infty$. Analysis of the master equations shows that

$$D=\tfrac{1}{3}h_r h_e/(h_r+h_e)$$

or, equivalently,

$$1/D=3(1/h_r+1/h_e). \tag{7}$$

Interpreting D as a ''conductance'' and thus $1/D$ as a ''resistance,'' the latter is analogous to a series resistance formula. This result is consistent with the feature that both hopping processes are necessary for long-range trimer diffusion. If $h_r=0$ but $h_e>0$, the trimer just cycles between the four configurations shown in the center of Fig. 3. In the artificial case where $h_e=0$ but $h_r>0$, the trimer can only rearrange and rotate about a pinned central atom.

In the regime of large h_e, there is a rapid cycling between four distinct bent configurations in the center of Fig. 3. Thus, as $h_e\to\infty$, we can replace these by a single quasiconfiguration, as indicated in Fig. 4 (top). Thus there remain two linear configurations and one quasi-configuration, so now $C=3$. Possible interconversions between these and associated rates are indicated in Fig. 4 (bottom). The rate $h_r/4$ is associated with the conversion of the quasi-configuration to a linear configuration by corner rounding because the former is in the required bent configuration only $\frac{1}{4}$ of the time. The rate h_r describes the reverse process. Analysis of the master equations yields $D=h_r/3$, consistent with Eq. (7).

Finally, we mention another way to directly visualize behavior in the limit $h_e\to\infty$. We note that the centers of mass of both horizontal and vertical linear configurations lie on the same square grid with lattice constant unity (as for the grid of atomic adsorption sites). The centers of mass of the quasiconfigurations lie on a second square grid with lattice constant unity, which interpenetrates the first. The center of mass can hop from the first grid to the second, randomly choosing any of four displacements $(\pm\frac{1}{2},\pm\frac{1}{2})$, each with rate h_r, and from the second to the first with the same displacements, each with rate $h_r/2$. (Thus, as $\tau\to\infty$, the second grid appropriately has twice the population of the first.) Analysis of this biased random walk process again produces $D=h_r/3$.

D. Tetramer diffusion

Here there are 19 configurations (one square, two linear, four T, four Z, and eight L shapes), so $C=19$. All these configurations occur with equal probability as $\tau\to\infty$, except for the square configuration, which is more highly populated by a factor of $\exp(\beta J)$. Straight edge diffusion, corner rounding, and core breakup are all operative. The latter is expected to be rate limiting and since typically $h_c\ll h_r$, one expects tetramer diffusion to be much slower than trimer diffusion (in our basic model).

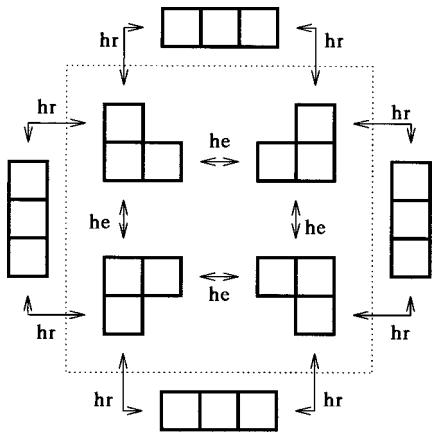

FIG. 3. Configurations and transition rates for trimer diffusion.

Because of the large number of configurations for the tetramer, we consider only the regime of large h_e, where there is rapid cycling between four L, two Z, and two T configurations. When $h_e\to\infty$, these eight configurations are replaced by a single quasiconfiguration, as indicated in Fig. 5 (top). This leaves one square, two linear, and two quasiconfigurations, so now $C=5$. Possible interconversions between these and associated rates are indicated in Fig. 5 (bottom). The rate $h_r/8$ applies for the conversion of the quasiconfiguration to a linear configuration by corner rounding because the former is in the required L configuration only $\frac{1}{8}$ of the time. The rate $h_r/4$ applies for conversion of the quasiconfiguration to a square configuration by corner rounding since the quasiconfiguration is in one of two required L configurations $\frac{1}{4}$ of the time. Conversion of a square configuration to either quasiconfiguration occurs at a rate $2h_c$ because there are two pathways involving core breakup. Quasiconfigurations interconvert by corner rounding at a rate $3h_r/8$ since they are in the required configurations $\frac{3}{8}$ of the time. Analysis of the master equations yields

$$D=6h_r h_c/(h_r+18h_c)$$

or, equivalently,

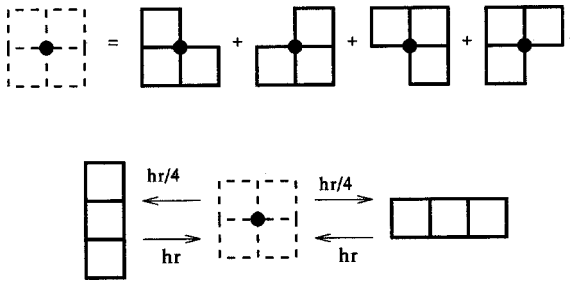

FIG. 4. Quasiconfiguration for bent trimers (top) and configurations and transition rates for the reduced description of trimer diffusion when $h_e\to\infty$ (bottom). The dot in this and several subsequent figures provides a fixed reference point.

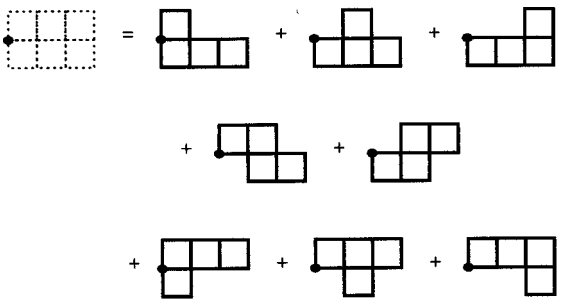

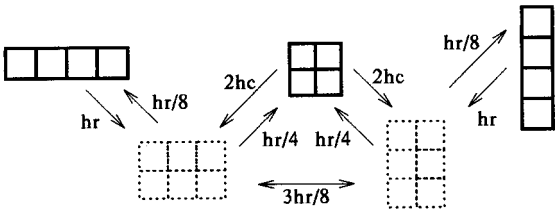

FIG. 5. Quasiconfiguration for tetramers (top) and configurations and transition rates for the reduced description of tetramer diffusion when $h_e \to \infty$ (bottom).

$$1/D = \tfrac{1}{6}[\,1/h_c + 18/h_r], \tag{8}$$

where the latter is analogous to a series resistance formula. This result shows that both core breakup and corner rounding are necessary for tetramer diffusion. In practice, one expects that $h_c/h_r = \exp(-\beta J) \ll 1$, so $D \approx 6h_c$.

There is a consistency issue to be considered here. We have assumed that h_r/h_e is negligibly small (or that h_e/h_r is very large) in applying the quasiconfiguration approach, but Eq. (8) retains corrections to $D \approx 6h_c$ of order $h_c/h_r = h_k/h_e = \exp(-\beta J)$. This is reasonable for $h_k \gg h_r$. However, if $h_k \approx h_r$ so h_r/h_e is comparable to h_c/h_r, then there may be comparable additional corrections to $D \approx 6h_c$ that must be determined from a full analysis with $C = 19$ configurations.

Finally, we note that while Eqs. (7) and (8) appear to be analogous series resistance formulas, there are basic differences between trimer and tetramer diffusion. For trimer diffusion, both straight edge hopping and corner rounding are necessary for the cluster to move an arbitrary distance. In contrast, tetramers can diffuse arbitrarily far through a sequence of nonsquare configurations, so core breakup is never invoked. However, tetramer diffusion is still controlled by core breakup since the noncompact cluster is guaranteed to ''fall into'' the square configuration, from which escape is mediated by core breakup.

E. Pentamer diffusion

A pentamer can assume the configuration of a square tetramer with an additional edge atom. One might therefore expect that true cluster diffusion would require disruption of the square core and thus be mediated by ''slow'' core breakup (the standard scenario for diffusion of large clusters).[6,8] However, an ''easy'' diffusion pathway exists for pentamers that avoids the necessity for direct core breakup, as was noted by Voter.[6] This pathway, which is shown in Fig. 6, demonstrates that pentamer diffusion is actually mediated by either corner rounding or kink escape, depending on which is less efficient (rather than by slow core breakup).

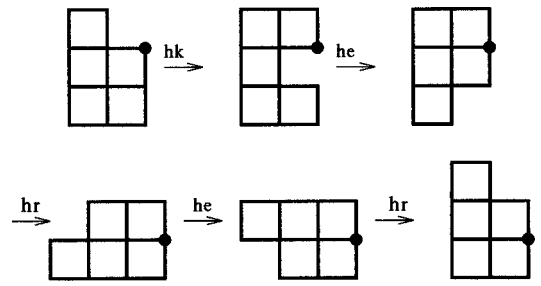

FIG. 6. Easy pathway for pentamer diffusion (see Ref. 6).

To simplify the analysis, we assume that h_r and h_k remain finite and consider the limiting regime where $h_e \to \infty$, which in turn requires that $h_c \to 0$ by virtue of detailed balance. We also neglect ''unfolding'' of the C-shaped configuration in Fig. 6 by corner rounding (immediately following kink escape) to obtain L-shaped and linear configurations. This is justified since straight edge diffusion is much more likely to follow kink escape (as shown in Fig. 6). Then there are just four quasiconfigurations of the pentamer, so $C = 4$. Each consists of a square tetramer core, with an additional atom confined to one side, as shown in Fig. 7 (top). Possible interconversions between these and associated rates are indicated in Fig. 7 (bottom). The rate $h_r/2$ applies for the conversion via corner rounding between one quasiconfiguration and another rotated by 90°, noting that the former is in the required configuration only $\frac{1}{2}$ of the time. The rate $h_k/2$ applies for the direct conversion mediated by kink escape between one quasi-configuration and another rotated by 180° (the first two steps in Fig. 6). Here there is a probability of $\frac{1}{2}$ that after the first kink escape steps, the pentamer returns to its original configuration rather than making the desired transition. Analysis of the master equations yields

$$D = \tfrac{1}{8} h_r h_k / (h_r + h_k)$$

or, equivalently,

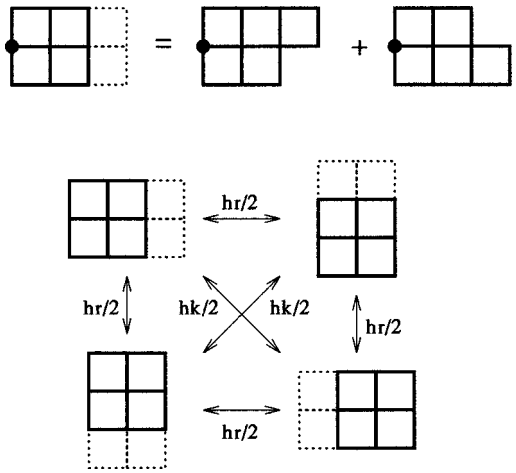

FIG. 7. Quasiconfiguration for pentamers (top) and configurations and transition rates for the reduced description of pentamer diffusion when $h_e \to \infty$ (bottom).

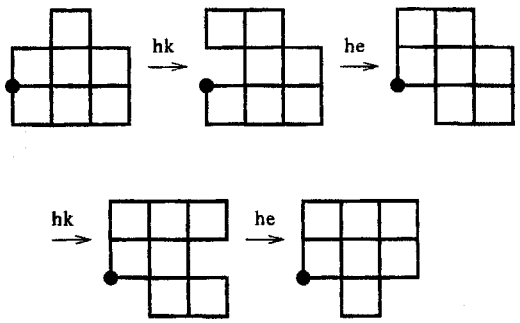

FIG. 8. First part of the easy pathway for septamer diffusion. Subsequent movement of the atom on the bottom edge to the center of the top edge recovers the original (but shifted) configuration.

$$1/D = 8(1/h_r + 1/h_k), \tag{9}$$

where the latter is analogous to a series resistance formula. This result is consistent with the feature evident from Fig. 6 that both corner rounding and kink escape are necessary for pentamer diffusion.

F. Diffusion of larger clusters

For *sexamer diffusion*, clearly core breakup is required to disrupt the rectangular 2×3 configuration and will thus mediate diffusion (as it does tetramer diffusion). We note that edge breakout is possible for the 2×3 sextamer configuration, unlike for smaller clusters. In general, this process must be incorporated in the modeling to ensure detailed balance (as is the case for larger clusters). However, in the limiting regime $h_b \ll h_c \ll h_r \approx h_k \ll h_e$, one can effectively ignore this edge breakout process since $h_b \ll h_c$. The reverse corner rounding process is correspondingly rare since the required initial five-bonded configuration has such a low population (even compared to the ''transient'' six-bonded configurations, which are accessed during diffusion by core breakup from the typical seven-bonded 2×3 configuration).

For *septamer diffusion*, the typical cluster configuration is a 2×3 rectangle with an additional edge atom. One might therefore expect that true cluster diffusion would require disruption of the rectangular core and thus be mediated by slow core breakup. In fact, an easy diffusion pathway exists, akin to that for pentamers, which just requires kink escape and corner rounding (as well as straight edge hopping). See Fig. 8.

For the *diffusion of larger clusters* that have typically near-square or near-rectangular configurations, breakup of the rectangular core at a rate h_c appears necessary and would thus mediate true long-range diffusion.[6,8] This is clearly the case for diffusion of octamers, nonamers, and decamers, which can be trapped in 2×4, 3×3, and 2×5 configurations, respectively. We note that it is often possible to move clusters arbitrarily far with a sequence of atomic hops not explicitly including core breakup. However, such motion invariably includes successive kink escape processes or kink escape and corner rounding processes, for which the effective rate is always comparable to or lower than that for core breakup (see below).

It is instructive to discuss the specific example of the evolution of a *decamer* starting from a 3×3 square configuration with an additional edge atom (a $3\times3+1$ configuration).

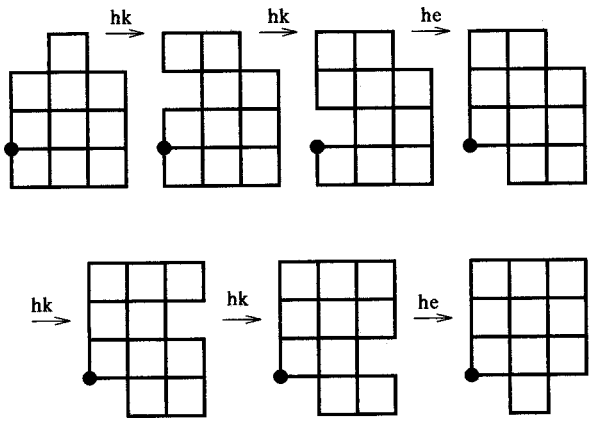

FIG. 9. First part of a pathway for decamer diffusion. Subsequent movement of the atom on the bottom edge to the center of the top edge recovers the original (but shifted) configuration. Due to successive kink escape processes, the effective rate is comparable to that for core breakup.

Motion of the additional atom around the periphery, mediated by corner rounding, cannot produce nonlocal cluster motion. However, nonlocal motion is possible through the sequence of moves not requiring core breakup, some of which are shown in Fig. 9. Despite this fact, the effective rate for the first two kink escape steps equals $\rho_{\rm eq} h_k$, where $\rho_{\rm eq} \approx \exp(-\beta J)$ gives the probability of finding the second configuration relative to the first. (From a kinetic perspective, after the first kink escape step, the atom is most likely to return to the kink via rapid edge hopping.) This effective rate is actually comparable to h_c. Note also that the decamer must eventually fall into a 5×2 configuration (which has the same configuration energy, and thus probability of occurrence, as the $3\times3+1$ configuration) and from which escape is mediated by core breakup.

V. RESULTS FOR CLUSTER DIFFUSION WITH CONCERTED MOTION OF ATOMS

A. Tetramer diffusion via ''dimer shearing''

Here we modify the basic model of tetramer diffusion in Sec. IV. We now incorporate an additional concerted dimer shearing process proposed by Shi *et al.*,[7] wherein a pair atoms on one side of a square tetramer shears at a rate h_s relative to the other pair to produce a Z-shaped configuration. For consistency, one must also incorporate the reverse shearing process with much larger rate h_s' satisfying the detailed-balance condition $h_s' = \exp(\beta J) h_s$. See Fig. 10.

We analyze this model only in the regime where h_e is much larger than all other rates. This is motivated by the expectation that $h_e \gg h_s' \gg h_r \approx h_k \gg h_s \gg h_c$. Thus, as $h_e \to \infty$, we can treat the eight L, Z, and T configurations in Fig.

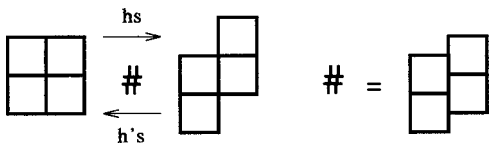

FIG. 10. ''Dimer shearing'' and ''reverse shearing'' of tetramers. # indicates the transition state.

5 (top) as a single quasiconfiguration and thus reduce the system to the same square, two linear, and two quasiconfigurations shown in Fig. 5 (bottom), so $C=5$. The only difference from the previous treatment of tetramer diffusion is the additional pathways for conversion between the square and quasiconfigurations. The rate $2h_s$ applies for conversion of the square configuration to a specific quasiconfiguration via dimer shearing since there are two possible pathways. The rate $h_s'/4$ applies for the reverse process since the cluster is in the required configuration $\frac{2}{8}$ of the time. Detailed analysis reveals that

$$D/h_s=\frac{1+13(h_r/h_s')+(h_c/h_s)+42(h_r/h_s')+13(h_r/h_s')(h_c/h_s)+42(h_r/h_s')^2(h_c/h_s)}{1+8(h_r/h_s')+18(h_s/h_s')+7(h_r/h_s')^2+126(h_r/h_s')(h_s/h_s')+18(h_c/h_s)(h_s/h_s')+126(h_r/h_s')(h_c/h_s)(h_s/h_s')}. \tag{10}$$

Imposing detailed-balance constraints on the rates in the above expression and setting $\mu=h_r/h_s'=h_c/h_s$, one obtains

$$D/h_s=\frac{1+14\mu+55\mu^2+42\mu^3}{1+8\mu+18\exp(-\beta J)+7\mu^2+144\mu\exp(-\beta J)+126\mu^2\exp(-\beta J)}. \tag{11}$$

Thus, in the regime where $\exp(-\beta J)\ll\mu\ll 1$, one has $D\approx h_s$.

As in the treatment of tetramer diffusion in Sec. IV, there is a consistency issue to be considered. We have assumed that h_s'/h_e is negligibly small (or that h_e/h_s' is very large) in applying the quasiconfiguration approach, but Eq. (10) retains corrections to $D\approx h_s$ of order $\mu=h_r/h_s'=h_c/h_s$ and also much smaller corrections. This is exact if h_k and h_e diverge relative to the other rates, but if $h_k\approx h_r$, there may be comparable additional corrections to $D\approx h_s$.

B. Diffusion of larger clusters

Here we briefly reconsider the diffusion of pentamers, sexamers, etc., accounting for possible concerted moves of more than one perimeter atom. It was already recognized by Shi *et al.*[7] that a dimer shearing process with a rate $h_s\gg h_c$ (see Sec. V A) would likely control the diffusion of sexamers and octamers, as well as the diffusion of tetramers. In analyzing the diffusion of other larger clusters, we are motivated to consider the possible role of concerted dimer edge hopping along straight edges at rate h_{de}, particularly given the expectation that $h_{de}\gg h_k$ based on semiempirical calculations.[7] Indeed, this rapid process with rate h_{de} can replace the first two steps (kink escape followed by straight edge hopping, with a much lower effective rate of $h_k/2$) in the easy pathway for pentamer diffusion (Fig. 6) and in that for septamer diffusion (Fig. 8). As a result, it is clear that pentamer and septamer diffusion via these easy pathways will be limited not by kink escape or dimer edge hopping, but rather by corner rounding at a rate h_r (cf. Ref. 7).

Next we consider again the evolution of a *decamer* from a $3\times3+1$ configuration, augmenting the discussion in Sec. IV F. We have already noted that with only single atom moves, nonlocal motion is controlled by an effective rate comparable to that for core breakup. However, dimer kink escape at a rate h_{dk}, followed by straight edge hopping [see Fig. 11(a)], can replace the first three steps in Fig. 9. From detailed balance one has $h_{dk}=\exp(-\beta J)h_{de}$ and since one might expect that $h_e\gg h_{de}\gg h_k\approx h_r\gg h_{dk}\gg h_c$, it follows that dimer kink escape can mediate evolution from this $3\times3+1$ configuration. Another possibility is trimer edge hopping along straight edges at a rate h_{te} [see Fig. 11(b)], which can also replace the first three steps in Fig. 9 and could also mediate this evolution since it is likely that $h_{te}\ll h_c$.

It should again be emphasized that eventually the decamer will fall into the 5×2 configuration (which should have similar configurational energy to the $3\times3+1$ configuration) and from which escape is presumably mediated by dimer shearing. Thus dimer shearing should also mediate overall decamer diffusion (unless dimer kink escape and trimer edge diffusion are slower). In this case, one would expect an activation barrier for decamer diffusion very close to that for octamers or sexamers, each of which is mediated by similar dimer shearing. However, experimental data for the $Rh_n/Rh(100)$ system[1] reveals a substantially lower activation

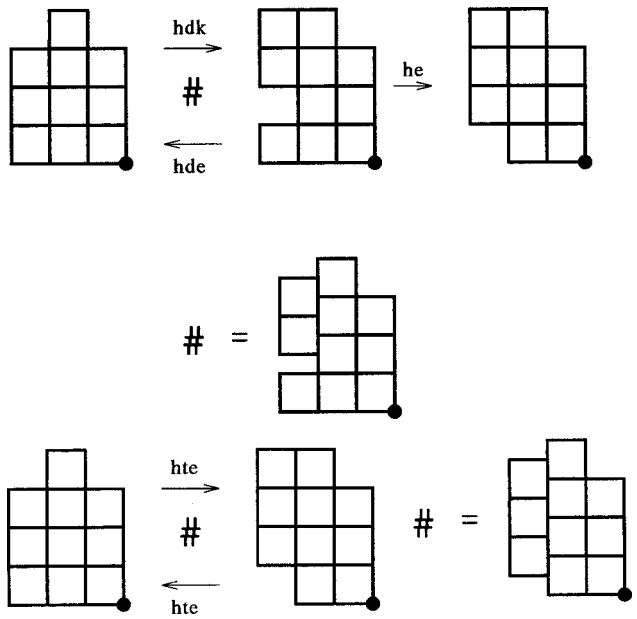

FIG. 11. Pathways for decamer evolution from the $3\times3+1$ configuration, which involves (a) dimer kink escape and (b) trimer edge hopping. # indicates the transition states.

barrier for decamer diffusion than for sexamer and octamer diffusion. This suggests that the 5×2 decamer configuration was not accessed in the experimental observation time, a speculation that has been confirmed by further analysis of the original experimental data.[15]

VI. CORRELATIONS IN THE MOTION OR WALK OF CLUSTERS

Diffusion of monomers and dimers, according to the model presented above, is described by a ''pure'' random walk, i.e., the mean-square displacement increases exactly linearly for all times, i.e., $\langle r^2\rangle = 4D\tau$ for all τ. However, for trimers and larger clusters, we shall see that the mean-square displacement typically increases ''more rapidly'' initially, before achieving a slower asymptotic linear increase satisfying $\langle r^2\rangle \sim 4D\tau$. The rapid initial increase is generally induced by the faster perimeter hopping processes. The long-range motion is mediated by a slower rate controlling process. Thus the ''time-dependent diffusion coefficient'' $D(\tau)=\langle r^2(\tau)\rangle/4\tau$ exhibits a *decrease* from an initial high value (controlled by the faster hop rates) to its lower asymptotic value of D. Such a decrease is the signature of a backward correlation in the cluster's walk.[8,12] Exact analytic determination of this behavior is possible using the formalism of Sec. III, but for convenience below we utilize kinetic Monte Carlo simulation techniques.

In the case of trimer diffusion with $h_e \gg h_r$, if one starts from a *bent* configuration, the center of mass will jump rapidly at a rate h_e between four locations, as the trimer cycles between four bent configurations (constituting the single quasiconfiguration discussed in Sec. IV). A simple calculation shows that $\langle r^2\rangle$ increases rapidly to around $\frac{1}{9}$ on a time scale of the order of $1/h_e$. Thereafter, the increase in $\langle r^2\rangle$ is slower on a time scale of order $1/h_r$, being mediated by corner rounding, so the overall behavior reflects a backward correlation (cf above). Starting from a *linear* configuration, one finds a roughly linear increase in $\langle r^2\rangle$ for all times (on a time scale of order $1/h_r$). Here this increase for very short times is already controlled by corner rounding and is actually slower than the asymptotic increase. Performing an equilibrium average over all initial configurations again yields backward correlation behavior. See Fig. 12. Finally, we note that a more comprehensive analysis of limiting behavior is possible using quasiconfiguration ideas.

Analogous and sometimes more complicated behavior is observed for larger clusters. In the case of tetramer diffusion with $h_e \gg h_r \gg h_c$, if one starts from an L, T, or Z configuration, the center of mass will jump rapidly at a rate h_e between that of eight configurations constituting a single quasiconfiguration discussed in Sec. IV. Thus $\langle r^2\rangle$ increases rapidly on a time scale of order $1/h_e$ to around $\frac{13}{64}$, $\frac{9}{64}$, and $\frac{5}{64}$ for initial L, T, and Z configurations, respectively. Then $\langle r^2\rangle$ will increase more slowly on a time scale of order $1/h_r$ as the tetramer makes transitions to linear and to L, T, and Z configurations not included in the initial quasiconfiguration, before eventually becoming ''trapped'' in a square configuration. Thereafter, the increase in $\langle r^2\rangle$ is slower, being mediated by core breakup. Distinct behavior is found starting with linear or square configurations.

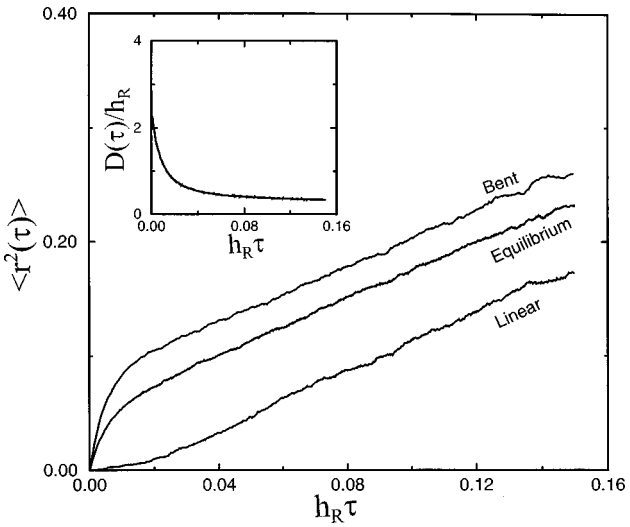

FIG. 12. Simulation study of trimer diffusion with $h_e/h_r = 100$ showing $\langle r^2(\tau)\rangle$ versus $h_r\tau$ for initially bent and linear configurations and for the equilibrium average initial configuration. The inset shows the behavior of $D(\tau)/h_r \to 100/303$ as $h_r\tau \to \infty$ for the latter.

VII. CONCLUSIONS

An exact analytic treatment of cluster diffusion of the type presented above in principle provides the most complete understanding of this phenomenon. Such studies quantify the role of competing kinetic pathways to diffusion (often exploiting series resistance or electrical network analogies[4,5]) and facilitate analysis of limiting regimes. We have shown that concerted adatom moves, which can sometimes control cluster diffusion (cf. Ref. 7), can also be incorporated. A fundamental problem remains in that the size or dimension of the analytic calculation is given by the number of cluster configurations, which increases exponentially with size. The introduction of quasiconfigurations in this work serves to reduce this dimension. Another strategy that we plan to consider in future work is to restrict the number of configurations of large clusters by limiting ''excitations'' about a near-square or near-rectangular shape.

ACKNOWLEDGMENTS

J.R.S. would like to acknowledge support from the International Institute of Theoretical and Applied Physics (IITAP) at Iowa State University (ISU). This work was supported by the NSF through Grant No. CHE-9700592. It was performed at Ames Laboratory, which is operated for the U.S. DOE by ISU under Contract No. W-7405-Eng-82.

APPENDIX: ACOUSTIC EIGENVALUE ANALYSIS FOR $\underline{\underline{M}}(\mathbf{k})$

To determine the acoustic eigenvalue of $\underline{\underline{M}}(\mathbf{k})$ it is sufficient to analyze the determinant[5]

$$\det[\underline{\underline{M}}(\mathbf{k})-\lambda\underline{\underline{I}}] \equiv \sum_{0\le n\le C} C_n(\mathbf{k})\lambda^n$$

since $\lambda_0(\mathbf{k}) \sim C_0(\mathbf{k})/C_1(\mathbf{k})$ as $k\to 0$. One can actually show that[5] $C_0(\mathbf{k}) = (-1)^C A_0 k^2 + O(k^4)$ and that $C_1(\mathbf{k}) = (-1)^C A_1 + O(k^2)$, so $D = A_0/A_1$. Determination of C_0

and C_1 and their Taylor expansions in $\mathbf{k}$ can be easily performed using MATHEMATICA. Again, here we set the surface lattice constant to unity.

1. Monomer diffusion

Here possible center-of-mass displacements are $\boldsymbol{\rho}=(\pm 1,0)$ or $(0,\pm 1)$, occurring with a rate h_0, and one has

$$M(\mathbf{k})=2h_0[\cos(k_x)+\cos(k_y)-2]=\lambda_0(\mathbf{k}),$$

so $A_0=h_0$, $A_1=1$, and $D=h_0$.

2. Dimer diffusion

Here possible center-of-mass displacements for transitions between horizontal and vertical configurations are $\boldsymbol{\rho}=(\pm\frac{1}{2},\pm\frac{1}{2})$, occurring with a rate h_r, and one has

$$\underline{\underline{M}}(\mathbf{k})=4h_r\begin{pmatrix} -1 & \cos(k_x/2)\cos(k_y/2) \\ \cos(k_x/2)\cos(k_y/2) & -1 \end{pmatrix},$$

so $A_0=4(h_r)^2$, $A_1=8h_r$, and $D=h_r/2$.

3. Trimer diffusion

Consider first the full analysis with four bent and two linear configurations, so $C=6$. See Fig. 3. Possible center-of-mass displacements for transitions between bent configurations in the center of Fig. 3 are $\boldsymbol{\rho}=(\pm\frac{1}{3},0)$ and $(0,\pm\frac{1}{3})$ and between bent and linear configurations are $\boldsymbol{\rho}=(\pm\frac{1}{3},\pm\frac{1}{3})$. Transition rates are also indicated in Fig. 3. We do not present the full 6×6 matrix $\underline{\underline{M}}(\mathbf{k})$, but just give the results of the determinant analysis in terms of $\Gamma=h_e/h_r$. One finds that

$$A_0=(h_r)^6[64\Gamma+192\Gamma^2+128\Gamma^2],$$

$$A_1=(h_r)^5[192+768\Gamma+960\Gamma^2+348\Gamma^3],$$

so $D=(h_r/3)\Gamma/(1+\Gamma)$.

We now turn to the simpler analysis for $h_e\to\infty$, where the four bent configurations are treated as a single quasiconfiguration, so with the two linear configurations one now has $C=3$. See Fig. 4. Possible center-of-mass displacements between the linear and quasiconfigurations are $\boldsymbol{\rho}=(\pm\frac{1}{2},\pm\frac{1}{2})$. Transition rates are indicated in Fig. 4. One has

$$\underline{\underline{M}}(\mathbf{k})=h_r\begin{pmatrix} -4 & 0 & \cos(k_x/2)\cos(k_y/2) \\ 0 & -4 & \cos(k_x/2)\cos(k_y/2) \\ 4\cos(k_x/2)\cos(k_y/2) & 4\cos(k_x/2)\cos(k_y/2) & -2 \end{pmatrix},$$

where the top two components correspond to the linear configurations and the bottom one to the quasiconfiguration. Thus one finds that $A_0=8(h_r)^3$ and $A_1=24(h_r)^2$, so $D=h_r/3$, consistent with the above general result in the $\Gamma\to\infty$ limit.

4. Tetramer diffusion

Here we consider only the simplified analysis for $h_e\to\infty$, with one square, two linear, and two quasiconfigurations, so $C=5$. See Fig. 5. Possible center-of-mass displacements for transitions between the square and quasiconfigurations are $\boldsymbol{\rho}=(\pm\frac{1}{2},0)$ and $(0,\pm\frac{1}{2})$ and between linear and quasiconfigurations are $\boldsymbol{\rho}=(\pm\frac{1}{2},\pm\frac{1}{2})$. Transition rates are also indicated in Fig. 5. Here, we do not present the full 5×5 matrix $\underline{\underline{M}}(\mathbf{k})$, but just give the results of the determinant analysis in terms of $\Lambda=h_r/h_c=\exp(\beta J)$. One finds that

$$A_0=168(h_c)^5\Lambda^4,\quad A_1=(h_c)^4\Lambda^3(28\Lambda+504),$$

so $D=6h_c\Lambda/(\Lambda+18)$.

5. Tetramer diffusion via dimer shearing

Here again we consider only the simplified analysis for $h_e\to\infty$, with the same configurations as for the above standard model of tetramer diffusion, so $C=5$. Thus we just include an additional pathway from square and quasiconfigurations via dimer shearing and for the reverse process via reverse shearing. We set $\Phi=h_s'/h_r$, $\Psi=h_s/h_r$, and $\vartheta=h_c/h_r$. Then a detailed analysis reveals that

$$A_0=(h_r)^5[4\Phi^2\Psi+52\Phi\Psi+4\Phi^2\vartheta+168\Psi+52\Phi\vartheta+168\vartheta],$$

$$A_1=(h_r)^4[4\Phi^2+32\Phi+72\Phi\Psi+28+504\Psi+72\Phi\vartheta+504\vartheta],$$

consistent with the above expressions for the standard model (upon setting $\Phi=\Psi=0$). These results yield the expression for D reported in the text.

6. Pentamer diffusion

Here we consider only the simplified analysis for $h_e\to\infty$ and $h_c\to\infty$ with four quasiconfigurations, so $C=4$. See Fig. 7. Possible center-of-mass displacements for transitions between the 180° rotated quasiconfigurations are $\boldsymbol{\rho}=(\pm\frac{3}{5},0)$ and $(0,\pm\frac{3}{5})$ and between 90° rotated quasiconfigurations are $\boldsymbol{\rho}=(\pm\frac{3}{10},\pm\frac{3}{10})$. Transition rates are also indicated in Fig. 7. We do not present the full 4×4 matrix $\underline{\underline{M}}(\mathbf{k})$, but just give the results of the determinant analysis in terms of $\Omega=h_k/h_r$. One finds that

$$A_0=(h_r)^4\Omega(1+\Omega)/4,\quad A_1=2(h_r)^3(1+\Omega)^2,$$

so $D=\frac{1}{8}h_r\Omega/(\Omega+1)$.

7. General comments

It is appropriate to note that further simplification is possible in some of the above analyses. Special features of the master equations can endow symmetries on the acoustic

eigenspace of $\underline{\underline{M}}(\mathbf{k})$ for arbitrary $\mathbf{k}$, thus leading dimensional reduction and simpler determination of $\lambda_0(\mathbf{k})$. For the dimer problem, both components of the acoustic eigenvector are equal, which immediately implies that $\lambda_0(\mathbf{k}) = 4h_r[\cos(k_x/2)\cos(k_y/2) - 1]$. For the full trimer problem, as well as for the simpler analysis incorporating a quasiconfiguration when $h_e \to \infty$, both components for linear trimers are equal.

*Permanent address: Facultad Ingenieria, Universidad Nacional de Mar del Plata, Avenida Juan B. Justo 4302, 7600 Mar del Plata, Argentina.

[1] G. L. Kellogg, Surf. Sci. Rep. **21**, 1 (1994); Phys. Rev. Lett. **73**, 1833 (1994).

[2] J. Villain, A. Pimpinelli, L. Tang, and D. Wolf, J. Phys. I **2**, 2107 (1992); S. Liu, L. Bonig, and H. Metiu, Phys. Rev. B **52**, 2907 (1995); M. C. Bartelt, S. Gunther, E. Kopatzki, R. J. Behm, and J. W. Evans, *ibid.* **53**, 4099 (1996).

[3] A. Masson, J. J. Metois, and R. Kern, in *Advances in Epitaxy and Endotaxy*, edited by H. G. Schneider and V. Ruth (VEB, Leipzig, 1971); S. Stoyanov and K. Kashchiev, Curr. Top. Mater. Sci. **7**, 69 (1981).

[4] D. A. Reed and G. Ehrlich, J. Chem. Phys. **64**, 4616 (1976); J. D. Wrigley, D. A. Reed, and G. Ehrlich, *ibid.* **67**, 781 (1977); U. Landman and M. F. Shlesinger, Phys. Rev. B **16**, 3389 (1977).

[5] U. M. Titulaer and J. M. Deutsch, J. Chem. Phys. **77**, 472 (1982).

[6] A. Voter, Proc. SPIE **821**, 214 (1986); Phys. Rev. B **34**, 6819 (1986).

[7] Z.-P. Shi, Z. Zhang, A. K. Swan, and J. F. Wendelken, Phys. Rev. Lett. **76**, 4927 (1996).

[8] J.-M. Wen, S.-L. Chang, J. W. Burnett, J. W. Evans, and P. A. Thiel, Phys. Rev. Lett. **73**, 2591 (1994); J.-M. Wen, J. W. Evans, M. C. Bartelt, J. W. Burnett, and P. A. Thiel, *ibid.* **76**, 652 (1996); C. R. Stoldt, A. M. Cadilhe, C. J. Jenks, J.-M. Wen, J. W. Evans, and P. A. Thiel, *ibid.* **81**, 2950 (1998); P. A. Thiel and Evans, in *Morphological Organization in Epitaxial Growth and Removal*, edited by Z. Zhang and M. G. Lagally (World Scientific, Singapore, 1998).

[9] W. W. Pai, A. K. Swan, Z. Zhang, and J. F. Wendelken, Phys. Rev. Lett. **79**, 3210 (1997).

[10] K. Morgenstern, G. Rosenfeld, B. Poelsma, and G. Comsa, Phys. Rev. Lett. **74**, 2058 (1995).

[11] S. V. Khare, N. C. Bartelt, and T. L. Einstein, Phys. Rev. Lett. **75**, 2148 (1995); C. DeW. Van Siclen, *ibid.* **75**, 1574 (1995); D. S. Sholl and R. Skodje, *ibid.* **75**, 3158 (1995); J. M. Soler, Phys. Rev. B **53**, R10 540 (1996); A. Bogicevic, S. Liu, J. Jacobsen, B. Lundqvist, and H. Metiu, *ibid.* (to be published).

[12] H. C. Kang, P. A. Thiel, and J. W. Evans, J. Chem. Phys. **93**, 9018 (1990); J.-M. Wen, J. W. Evans, S.-L. Chang, J. W. Burnett, and P. A. Thiel, in *Evolution of Thin-Film and Surface Structure and Morphology*, edited by B. G. Demczyk, E. D. Williams, E. Garfunkel, B. L. Clemens, and J. E. Cuomo, MRS Symposia Proceedings No. 355 (Materials Research Society, Pittsburgh, 1995), p. 15.

[13] From Eq. (4) one has $P_s(\tau) \to \exp(-\beta E_s)/Z + O(\exp(-r\tau))$, as $\tau \to \infty$, where $r = \min|\lambda_{i>0}(\underline{0})|$. This rate is controlled by the slowest atomic hop rate limiting transitions between configurations.

[14] Our direct derivation of the diffusion coefficient from the master equation shows that it is unnecessary to invoke the Chapman-Enskog approach, as done in Ref. 5.

[15] G. L. Kellogg (private communication). Note also that data for $Rh_n/Rh(100)$ suggests a barrier for ''dimer shearing'' in tetramers substantially below that for sexamers and octamers.